Published in final edited form as:
J Am Chem Soc. 2008 June 25; 130(25): 8069–8078.

Enantiomer-specific binding of ruthenium(II) molecular wires by the amine oxidase of *Arthrobacter globiformis*

David B. Langley[†], **Doreen E. Brown**[‡], **Lionel E. Cheruzel**[#], **Stephen M. Contakes**[#,≠], **Anthony P. Duff**[†,¶], **Kimberly M. Hilmer**[‡], **David M. Dooley**[*,‡], **Harry B. Gray**[*,#], **J. Mitchell Guss**[*,†], and **Hans C. Freeman**[*,†]

†*School of Molecular and Microbial Biosciences, University of Sydney, NSW 2006, Australia*

‡*Department of Chemistry and Biochemistry, Montana State University, Bozeman, MT 59717, USA*

#*Beckman Institute, California Institute of Technology, Pasadena, CA 91125, USA*

Abstract

The copper amine oxidase from *Arthrobacter globiformis* (AGAO) is reversibly inhibited by molecular wires comprising a Ru(II)-complex head group and an aromatic tail group joined by an alkane linker. The crystal structures of a series of Ru(II)-wire-AGAO complexes differing with respect to the length of the alkane linker have been determined. All wires lie in the AGAO active-site channel, with their aromatic tail group in contact with the trihydroxyphenylalanine quinone (TPQ) cofactor of the enzyme. The TPQ cofactor is consistently in its active ('off-Cu') conformation, and the side chain of the so-called 'gate' residue Tyr296 is consistently in the 'gate-open' conformation. Among the wires tested, the most stable complex is produced when the wire has a $-(CH_2)_4-$ linker. In this complex, the Ru(II)(phen)$(bpy)_2$ head group is level with the protein molecular surface. Crystal structures of AGAO in complex with optically pure forms of the 'C_4' wire show that the linker and head group in the two enantiomers occupy slightly different positions in the active-site channel. Both the Λ and Δ isomers are effective competitive inhibitors of amine oxidation. Remarkably, inhibition by the 'C_4' wire shows a high degree of selectivity for AGAO in comparison with other copper-containing amine oxidases.

Introduction

Copper amine oxidases catalyze the oxidative deamination of primary amines to the corresponding aldehyde. Their catalytic site contains a Cu atom and an organic cofactor, trihydroxyphenylalanine quinone (TPQ) (Figure 1). A channel connects the active site to the molecular surface. The Cu amine oxidase of the bacterium *Arthrobacter globiformis* (AGAO) has been used to study the effect of molecular 'wires' designed to fit into the active-site channel. Such wires typically have a 'tail' group that makes contact with the active site, a 'head' group that lies close to the surface of the protein, and a linker that joins them. For example, wires with a thiol head group can provide a conducting link between the enzyme active site and a gold electrode, thus enabling the electrochemistry of the active site to be explored.[1] Other wires, which were originally designed to demonstrate the pathway by which substrates reach the active site, have been useful in probing mechanisms of inhibition. In wires of the latter class, a dimethylaniline (DMA) tail group is linked to a $[Ru(phen)(bpy)_2]^{2+}$ head group by an alkane chain (Scheme).[2] The DMA–$(CH_2)_n$–$[Ru(phen)(bpy)_2]^{2+}$ wires are potent AGAO

Email: dmdooley@montana.edu; hgcm@its.caltech.edu; m.guss@mmb.usyd.edu.au; freemanh@chem.usyd.edu.au.
≠Present address: Chemistry Department, Westmont College, Santa Barbara, CA 93108, USA
¶Present address: ANSTO Institute for Environmental Research, Menai, NSW 2234, Australia

inhibitors, with a potency that decreases with the length *n* of the linker.[2] Our hypothesis was that by optimizing the interactions of the head group, the linker, and the active-site recognition element (tail group) with the enzyme, wires could be obtained that selectively inhibit AGAO in the presence of other amine oxidases. If successful, this approach may lead to the rational design of molecular wires that selectively inhibit amine oxidases in therapeutically relevant contexts.

We have made progress toward this goal by determining the crystal structure of the complex between AGAO and [DMA–$(CH_2)_4$–Ru(phen)$(bpy)_2]^{2+}$.[2] In this complex, the wire occupies the hydrophobic channel to the active site, the DMA tail group is in contact with the TPQ cofactor, and the Ru head group lies at the molecular surface. The structure analysis left three features for further study. First, the electron density of the linker between the DMA and [Ru(phen)$(bpy)_2]^{2+}$ groups was discontinuous. Second, the electron density at the Ru head group was not sufficiently strong and defined to permit the phen and bpy ligands to be modelled. Third, electron-density and anomalous scattering difference maps consistently had two peaks attributable to the Ru atom, instead of the expected single peak. Since [Ru(phen)$(bpy)_2]^{2+}$ is chiral, and since the crystals were prepared with a racemic mixture of the wire enantiomers, it was suggested that the Ru atom occupies slightly different positions depending on its chirality.

We now report high-resolution structures of two AGAO-wire complexes prepared from purified enantiomers of the [DMA-$(CH_2)_n$-Ru(phen)$(bpy)_2]^{2+}$ wire with $n = 4$ and structures of AGAO-wire complexes with longer linkers (*n* between 5 and 11). In addition, we report the results of kinetics experiments comparing both the resolved enantiomers and the racemate of [DMA-$(CH_2)_4$-Ru(phen)$(bpy)_2]^{2+}$ as inhibitors of AGAO and four other copper-containing amine oxidases. Taken together, the findings shed new light on the factors controlling the recognition of these unique inhibitors by bacterial amine oxidases.

Materials and Methods

Preparation of molecular wires: General

The racemic DMA-C_n-Ru(phen)$(bpy)_2$ wires with $n = 5$, 6, 7, 9 and 11, as well as the ligand 4-(m-$(CH_2)_4$-$OC_6H_4NMe_2$)-phen, were prepared by published methods.[2] The preparation of the Λ- and Δ-C_4 wires was based on a procedure developed by Hua and von Zelewsky for [Ru(phen)$(bpy)_2]X_2$.[3] Enantiomeric tartrate salts of $[Ru(bpy)_2py_2]^{2+}$, [Λ-Ru$(bpy)_2py_2$][(−)-O,O-dibenzoyl-L-tartrate].$12H_2O$ and [Δ-Ru$(bpy)_2py_2$][(+)-O,Odibenzoyl-D-tartrate].$12H_2O$, were isolated as single crystals. Reaction of the tartrate salts with 4-(m-$(CH_2)_4$-$OC_6H_4NMe_2$)-phen then yielded the enantiomeric C_4 wires. Details of the procedures are given below. The CD spectra of 58–59 μM solutions in MeCN (A_{456} = 0.90–0.92) were recorded on an Aviv Model 62A spectropolarimeter. The enantiomeric purity of the Λ- and Δ-enantiomers was estimated as ≥90% by comparing the CD spectra (Figure S1, Supplementary Information) with that of [Λ-Ru(phen)$(bpy)_2]X_2$.[3] All manipulations involving enantiopure ruthenium complexes and reagents were performed in the dark under an argon atmosphere.

(Λ-Ru$(bpy)_2$[4-(m-$(CH_2)_4$-$OC_6H_4NMe_2$)-phen])$(NO_3)_2$

A mixture of 0.40 g (0.33 mmol) [Λ-Ru$(bpy)_2py_2$][(−)-O,O-dibenzoyl-L-tartrate].$12H_2O$ and 148 mg (0.4 mmol) 4-*m*-$(CH_2)_4$-$OC_6H_4NMe_2$-phen in 10 mL 10/90 (v/v) H_2O/ethylene glycol was heated to 120 °C for 5 h. The reaction mixture was allowed to cool, and water (150 mL) was added to precipitate the crude product as an orange solid. The crude solid was purified by silica chromatography (2 × 40 cm) using KNO_3-saturated 10/10/80 (v/v) H_2O/EtOH/MeCN as eluant. The product was eluted as the first red band off the column. Solvent was removed under an oil-pump vacuum and the product was extracted from the resulting residue by two 10 mL portions of CH_2Cl_2. The CH_2Cl_2 solution was concentrated under vacuum to ~2 mL and

the product was precipitated by addition of 20 mL Et_2O. Yield: 0.268 g (85%). The identity of the product was confirmed by UV, ^1H NMR, and ESI-MS, giving parameters virtually identical with those reported previously for the racemate: ^1H NMR (300 MHz, CD_3OD): δ 1.85-2.05 (m, 6H), 2.9 (s, 6H), 4.06 (t, J=5.7 Hz, 2H), 6.21-6.24 (m, 2H), 6.35 (ddd, J=7.8,1.8, 0.5 Hz, 1H), 7.05 (m, 1H), 7.30 (m, 2H), 7.53 (m, 2H), 7.61 (m, 2H), 7.72 (d, J=5.5 Hz, 1H), 7.81 (dd, J = 8,5 Hz, 1H), 7.93 (d, J=5.5 Hz, 2H), 8.0-8.1 (m, 3H), 8.12-8.2 (m, 3H), 8.29 (d, J=9 Hz, 1H), 8.51 (d, J= 9 Hz,1H), 8.58 (dd, J = 7,0.7 Hz, 1H), 8.7 (m, 3H). ESI-MS (MeOH) m/z: 847 (M-NO_3^+), 784 (M-2NO_3-H^+). CD (58 μM in MeOH):$\Delta\varepsilon_{420\ nm}$ = −13.4 m° M^{-1} cm^{-1}, $\Delta\varepsilon_{472\ nm}$ = +11.4 m° M^{-1} cm^{-1}.

(Δ-Ru(bpy)$_2$[4-(m-(CH$_2$)$_4$-OC$_6$H$_4$NMe$_2$)-phen])(NO$_3$)$_2$

A mixture of 0.060 g (0.049 mmol) [Δ-Ru(bpy)$_2$py$_2$][(+)-O,O-dibenzoyl-D-tartrate].12H_2O and 22 mg (0.06 mmol) 4-*m*-(CH$_2$)$_4$-OC$_6$H$_4$NMe$_2$-phen in 10 mL 10/90 (v/v) H_2O/ethylene glycol was heated to 120 °C for 5 h. The reaction mixture was allowed to cool, water (150 mL) was added, and the crude product was collected by washing on a 3 cm silica gel plug. The product was eluted as the only red band using KNO_3-saturated 10/10/80 (v/v) H_2O/EtOH/MeCN. Solvent was removed under an oil-pump vacuum, and the product was extracted from the resulting residue by two 10-mL portions of CH_2Cl_2. The CH_2Cl_2 solution was concentrated under vacuum to ~2 mL, and the product was precipitated by addition of 20 mL Et_2O. Yield: 0.023 g (50%). The identity of the product was confirmed by UV, ^1H NMR, and ESI-MS, giving parameters virtually identical with those reported previously for the racemate and Λ-isomer. CD (59 μM in MeOH): $\Delta\varepsilon_{420\ nm}$ = +15.9 m° M^{-1} cm^{-1}, $\Delta\varepsilon_{472\ nm}$ = −13.8 m° M^{-1} cm^{-1}.

Co(bpy)$_2$[4-(m-(CH$_2$)$_4$-OC$_6$H$_4$NMe$_2$)-phen])(NO$_3$)$_3$

A solution of 53 mg (0.10 mmol) [Co(bpy)$_2$Cl$_2$]Cl in 100 mL EtOH was treated by addition of 51 mg (0.3 mmol) $AgNO_3$ and heated at reflux for 4 h. The resulting suspension was filtered through a 1 cm Celite plug to remove AgCl precipitate. The filtrate was treated with 37 mg (0.10 mmol) 4-(*m*-(CH$_2$)$_4$-OC$_6$H$_4$NMe$_2$)-phen, degassed, and heated at reflux for 4 h. The solvent was removed to give the crude product as a tan powder, which was purified by silica gel chromatography using 1/1/98-10/10/80 (v/v/v) KNO_3 saturated H_2O/EtOH/MeCN as the eluant. The product eluted as the main yellow band. Yield: 12 mg (12%). ESI-MS (m/z): 863 ([Co(bpy)$_2$phenC$_4$OmDMA](NO$_3$)$_2^+$), 401 ([Co(bpy)$_2$phenC$_4$OmDMA](NO$_3$)$^{2+}$]). UV-vis (25/75 (v/v) H_2O/EtOH) λ(ε): 268 (84,000), 348 nm (2,400 $M^{-1}cm^{-1}$).

Crystallization of AGAO, and formation of AGAO-wire complexes

AGAO was purified as described previously.[4] Crystals of AGAO were grown by the hanging-drop vapor diffusion method. Each drop contained protein (2 μL, 10 mg/mL) and an equal volume of a well solution comprising ammonium sulfate (0.6–1.1 M) and Na citrate (0.15 M), pH 6–7.5. Crystals appeared after several weeks at ambient temperature (22°C). Cryoprotection of the crystals and addition of wire were performed simultaneously, as follows: Well solution was added gradually to the drop until the drop volume reached 20 μL. The drop was transferred to a sitting-drop platform and the volume was increased to 30 μL. Half of the solution was then replaced step-wise with a series of well solutions containing a >10-fold stoichiometric excess of wire and 5% increments of glycerol. This step was carried out 12 times, twice for each increment in glycerol concentration from 5 to 30% v/v. The equilibrations were generally performed over a 24-h period, with the first equilibration taking at least 12 h. Practical considerations prevented the use of strictly identical procedures for the various AGAO-wire complexes. The crystals were flash frozen in a stream of N_2 gas at 100 K.

X-Ray data

Diffraction images were recorded on a Mar345 image-plate detector using Cu K_α X-rays (λ= 1.5418 Å) from an in-house Rigaku RU-200 rotating anode generator with Osmic mirror optics (Auburn Hills, MI, USA). Diffraction data were indexed and scaled using the HKL software suite.[5]

Crystal structure refinements

The starting model for the refinement of all the structures was the native AGAO structure refined at 1.55 Å resolution.[6] The model was first stripped of solvent, metal ions, sulfate ions and glycerol molecules. Residues with multiple conformers were assigned zero occupancy. The active-site TPQ (residue 382) was replaced by alanine. Initial low-resolution rigid-body refinement was followed by rounds of restrained refinement with TLS (translation, libration and screw-motion) parameterization[7] alternating with the inspection of electron-density maps and manual adjustment of the model. The Cu atom was added early in the refinement, as were solvent molecules displaying good electron density and reasonable stereochemistry. Solvent molecules near the active-site channel were added later. Alternate amino-acid conformers, exogenous sulfate ions and glycerol molecules were added last, if warranted by omit maps. The TPQ cofactor was clearly defined in an 'off-Cu' conformation, and was inserted in place of Ala382.

The wire molecule was left un-modelled in each refinement until its position was revealed by strong (though not necessarily continuous) F_{obs}-F_{calc} electron density. This generally occurred at an advanced stage of the refinement. In the two structures containing the Λ and Δenantiomers of the n = 4 wire, continuous electron density unambiguously revealed the DMA group, the –$(CH_2)_4$– linker, and the Ru(phen)$(bpy)_2$ group. In the case of the wires with n = 5, 6, 7, 9 and 11, there were two prominent electron-density features: one was adjacent to the TPQ, and represented the DMA group, while the other was in a plausible position for the Ru atom. The identification of the latter feature as representing the Ru atom was confirmed by peaks in anomalous scattering difference maps. However, the electron density between the DMA group and the Ru atom was either consistently weak and discontinuous, or non-existent. A wire, arbitrarily chosen to have a Λ head group, was modelled into these features with a linker of appropriate length, and was refined. The electron-density difference and anomalous scattering difference maps of the wires with n = 5, 6, 7 and 9 all had a weaker second Ru peak, which was modelled as the Ru atom of a second conformer. Since the chirality of neither Ru head group was known, the Λ chirality was retained. The occupancies of the DMA group and the Ru atom in each wire were varied systematically until the residual electron density was minimized.

The anomalous scattering difference maps mentioned above were used to make semi-quantitative comparisons among the various wire complexes. A typical map had peaks at the positions of the Cu atom, well-resolved S atoms, and the Ru atom. The peak representing the S atom of Met441 was used as a standard, since the side chain of this residue is very well ordered in all the structures. The amplitudes of the other anomalous difference peaks were then expressed as a fraction of the amplitude of the S(Met441) peak. The S(Met280) atom was represented by two weak peaks consistent with the presence of two side-chain conformers, and the amplitude of the weaker peak gave an indication for the threshold of significance of other features in the maps.

The X-ray data and refinement statistics are set out in Table 1, and the relative amplitudes of anomalous scattering peaks are given in Table 2. The coordinates and structure factors of the structures have been deposited in the Protein Data Bank. Monomer libraries for the Ru(II)phen-C_n-DMA wires were constructed using a combination of P_{RODRG},[7] the CCP4 molecular library

sketcher,[8] and manual parameter adjustment. Crystallographic refinement was carried out with REFMAC5.[9] The final structures were validated by using PROCHECK[10] and MOLPROBITY.[11] Figures were constructed with PYMOL.[12]

Inhibition experiments

Kinetics assays and absorption spectra were collected either on a Varian Cary 6000i scanning UV/Vis/NIR spectrophotometer equipped with a dual cell Peltier accessory for temperature control, or on an HP8453 photodiode array spectrophotometer equipped with a circulating temperature bath. Protein concentrations were determined using previously published extinction coefficients based on 280 nm absorbances for recombinant AGAO,[13] and for native sources of ECAO (*E.coli* amine oxidase),[14] PSAO (pea seedling amine oxidase),[15] PPLO (*Pichia pastoris* lysyl oxidase),[16] and BPAO (bovine plasma amine oxidase).[17] Activities were determined in triplicate at each concentration of benzylamine by monitoring the production of benzaldehyde at 250 nm (ε= 12,800 $M^{-1}cm^{-1}$) over 3 min (25 °C).[18,19] For a typical assay, a 5–10 μL aliquot of enzyme was diluted into 0.1 M potassium phosphate buffer (pH 7.2) containing the appropriate amount of inhibitor (3 mL total volume) and incubated for 1 min. The final protein concentrations for the AGAO assays were 0.021 μM (racemic and Λ wires) and 0.037 μM (Δwire), the difference reflecting the volume and concentration of the original aliquot of stock solution. The cuvette was inverted 3 times to ensure proper mixing, benzylamine was added to the sample, the cuvette was inverted again, and kinetics were then monitored. Stock solutions of inhibitor were prepared in 0.1 M potassium phosphate buffer (pH 7.2) or doubly-deionized water, and concentrations were determined using ε_{452} = 14,500 M^{-1} cm^{-1} at 452 nm.[2] Control assays were performed throughout the course of each curve to verify the stability of the inhibitors. Inhibitor solutions were kept on ice and wrapped in aluminum foil to avoid degradation. In experiments using ECAO, assays were run at 37 °C (1 ml total volume). In the case of BPAO, 700 units of beef liver catalase (Boehringer Mannheim) were added to each assay to prevent any inactivity of the protein due to product H_2O_2.[20] A stock solution of catalase was prepared in 0.1 M KPO4 pH 7.2 buffer and kept on ice during the course of the experiment. In assays with the $Co(bpy)_2$[4-(*m*-$(CH_2)_4$-$OC_6H_4NMe_2$)-phen]) $(NO_3)_3$ wire, inhibitor concentrations were determined using an ε_{268} = 86000 M^{-1} cm^{-1}. The wire compound was dissolved in a 3:1 (v/v) EtOH/H_2O solvent. Final protein concentration in the assay was 0.027 μM. Kinetics data were analyzed using a statistical software package (GraphPad Prism, San Diego, CA). User-defined models for competitive, non-competitive, uncompetitive, and mixed-type inhibition as described by Segel[21] were entered into GraphPad. Fits were established by global nonlinear regression analyses. The inhibition constants were derived from the best-fit parameters.

Results

AGAO-wire complexes crystallize in two types of unit cell

As stated in ‘Materials and Methods’, crystals of AGAO-wire complexes were prepared by ‘soaking’, i.e., by adding a solution of wire to the solution surrounding an AGAO crystal. The AGAO crystal chosen for each experiment was the best available at the time. As a result, the complexes are distributed over two of the four known crystal forms of AGAO.[6] All the racemic complexes, including the racemic AGAO-C_4-wire complex reported previously, were prepared from AGAO crystals of ‘form II’, whereas the two new complexes with enantiopure n = 4 wires belong to ‘form IV’. Crystals of ‘form II’ have only half of the AGAO homodimer (one protomer) in the asymmetric unit. Crystals of ‘form IV’ have a larger unit cell, and their asymmetric unit includes an entire AGAO dimer (two protomers). The structures of the Λ- and Δ-C_4-wire complexes in ‘form IV’ crystals were refined without non-crystallographic symmetry restraints, so that they provide two crystallographically independent examples of the structure. In the event, there are only small differences between the structures of the two

crystallographically independent protomers in both the Λ– and Δ–C_4-wire complexes. Where our description of these complexes appears to refer to a single structure, it is in fact based on two independent sets of observations.

Structures of AGAO complexes with enantiomers of the C_4 wire

In the structure analyses of the AGAO complexes with the Λ- and Δ-enantiomers of the $n = 4$ wire, continuous electron density unambiguously revealed the DMA tail group, the -$(CH_2)_4$- linker, and the Ru(phen)$(bpy)_2$ head group (Figure 2). The positions of the DMA group with respect to the TPQ were effectively identical in the enantiomeric structures (Supplementary Table S1). The C_4 linker followed slightly different paths along the channel. The chiral head group was observed clearly in both structures, the phen and bpy molecules being defined better in the Λ structure where the occupancy of the head group was higher (Table 2). In both protomers of the Λ structure, the position of the Ru atom was confirmed by a single large anomalous scattering difference peak. In one protomer, a second but much smaller impurity peak occurred at a position corresponding to the main Ru peak in the Δ structure. Conversely, in both protomers of the Δ structure, the major anomalous peak was accompanied by a minor peak attributable to the Ru atom in the Λ enantiomer.

Stereospecific interactions in the active-site channel

The electron-density maps and models of the C_4 wires were sufficiently clear to permit observations on the fit between the linkers and the active-site channel. The side chains of three residues near the entrance to the channel – Glu102, Phe105 and Leu358 – have different conformations in the complexes with the Λ- and Δ- wires (Figure 3). The two conformers of Glu102 have different torsion angles about the C^{β}–$C^{\gamma}$and C^{γ}–C^{δ} bonds, with the result that the positions of corresponding atoms in the carboxylate group differ by 1–2 Å. The movements of Phe105 and Leu358 are more pronounced. Phe105, the residue adjacent to Glu102 in the channel, points away from the channel in the complex with the Λ wire, but into the channel in the complex with the Δ wire. The first conformer has not been observed previously, while the second is similar to those found in other structure analyses of AGAO. The side chain of Leu358, which is now resolved in two conformations, was unresolved in previous structure analyses of AGAO.

Comparisons between the Λ- and Δ-C_4 wire complexes and native AGAO

Two observations are particularly relevant to rationalizing the interactions between the wires and AGAO. The first is the formation of a hydrogen bond between the O4 atom of the TPQ and the hydroxyl group of a conserved tyrosine, Tyr284 (Figure 4). This bond, which is not present in native AGAO structures,[6] helps to stabilize the conformation of the TPQ cofactor in the presence of a C_4 wire. The second observation concerns Tyr296, which has been described as a ‘gate’ to the active site. In the structures where a C_4 wire is bound, the side chain of Tyr296 nestles in a hydrophobic depression between Leu137 and Gln294 (Figure 4). In this conformation, the gate is ‘open’. In native AGAO structures, the side chain of Tyr296 projects into the channel, and the gate is said to be ‘closed’. In the closed-gate conformation, the hydroxyl atom O^{η} (Tyr296) is hydrogen bonded to the first of a chain of four water molecules in the active-site pocket and channel. There is an additional water molecule in the space that will be occupied by the aromatic ring of Tyr296 when the gate opens. Thus, at least five crystallographically identified water molecules must be displaced when the conformation of the Tyr296 gate changes from ‘closed’ to ‘open’.

Structures of AGAO complexes with racemic C_5-C_{11} wires

When AGAO was complexed with the racemic C_5-, C_6-, C_7-, C_9- and C_{11}-wires, the electron-density maps had the same general features as observed earlier in the structure of the racemic

C_4-wire complex.[2] The electron density of the DMA group was consistently well resolved and in essentially the same position as in the enantiopure C_4 wire complexes. In contrast, the electron density of the linker was weak and discontinuous, and the Ru head group was represented by either one or two strong electron-density peaks. The latter peaks were confirmed as Ru by being superposed on peaks in an anomalous scattering difference map (Figure 5). They lay close to the protein surface at or outside the entrance to the active-site channel, and presumably indicated the preferred position of Ru head groups with opposite chiralities. At the AGAO active site, the TPQ cofactor was consistently ordered in the 'off-Cu' conformation (Figure 4).

Three qualitative trends in the structures of the complexes with the C_5-C_{11} wires were noted. As the length of the wires increased, there was (with one irregularity) a systematic increase in the distance from the TPQ to the Ru peak(s) (Table 3), the quality of the wire electron density decreased, and the amplitude of the Ru peaks decreased (Table 2). The significance of these trends is mentioned later.

Inhibition experiments

The racemic mixture of the C_4 wire is known to be a potent inhibitor of benzylamine oxidation by AGAO.[2] The present work shows that the resolved Λ- and Δ-isomers are also effective: the K_i values from the global fits are 27 ± 1 nM (racemic); 36 ± 2 nM (Δ); and 32 ± 1 nM (Λ), demonstrating little or no stereocontrol (Table 4, Figure 6). A competitive inhibition model (*versus* benzylamine) best accounts for the data for the three wires ($R^2 \geq 0.995$).

Significantly higher K_i values were determined for the inhibition of benzylamine oxidation using the C_4 wires with *all* other amine oxidases. While a competitive mode of inhibition was observed for ECAO with both isomers, the K_i values were an order of magnitude larger compared with AGAO (Table 4). Further, greater enantioselectivity was observed for ECAO: the Λ isomer was ~4x more effective than the Δ-isomer (K_i values = 0.27± 0.02 μM (Λ) and 1.10 ± 0.08 μM (Δ), $R^2 \geq 0.992$, data not shown) The racemic C_4 wire was dramatically less effective against BPAO, with the data best described by a non competitive fit with K_i = 44 ± 4 μM (R^2 = 0.973). *No inhibition* was observed for the same wire screened against either PSAO or PPLO (data not shown).

It is likely that the observed inhibition patterns reflect the competition, under turnover conditions, between the inhibitor and substrate for the free enzyme (E) and the enzyme-substrate complex (ES) (see Lineweaver-Burk plots, Supplementary Figure S2). We note that the strongest inhibition is also competitive, implying that the inhibitor binds sufficiently well to preclude substrate binding to E. Mixed and non-competitive inhibitions imply that the inhibitor binds to both E and ES ("mixed") or only to ES ("non-competitive"). Pure "non-competitive" inhibition with the inhibitor binding exclusively to the ES complex is rare, and probably represents a limiting case of mixed inhibition, where inhibitor binding to the free enzyme E makes only a minor contribution.

To assess whether the charge of the head group could influence AGAO inhibition by the C_4 wire, the Co^{III} analogue, $(Co^{III}(bpy)_2[4\text{-}(m\text{-}(CH_2)_4\text{-}OC_6H_4NMe_2)\text{-}phen])(NO_3)_3$ was evaluated. The Co^{III} wire was an effective inhibitor but slightly *less* potent than the Ru^{II} C_4 wire, despite the increased positive charge. A mixed-type inhibition model best described the data, with a K_i of 120 ± 4 nM (R^2 = 0.996) (Table 4, Figure 7).

Discussion

Overview of the AGAO complexes with the enantiomeric C_4 wires

The preparation of the optically pure enantiomers of the C_4 wire, Λ- and Δ-[DMA-C_4-Ru(II)(phen)$(bpy)_2$], has made it possible to prepare AGAO complexes with a single species of wire molecule, instead of the two species that are present in a racemic mixture. The resulting crystal structures of the AGAO complexes with the Λ- and Δ-C_4 wires are less affected by disorder, and yield the most detailed models so far for the interactions between the wire and the protein.

At the head-group end of the wire, the structures confirm that the position of the Ru atom in relation to the protein molecule depends on the chirality of the Ru(phen)$(bpy)_2$ moiety. This was one of the key hypotheses in the earlier description of the racemic AGAO-C_4-wire complex, where the Ru atom seemed to be represented by two peaks in electron-density maps and in anomalous scattering difference maps.[2] It is now clear that the two peaks indeed corresponded to the Ru atom in the two enantiomeric components of the racemic C_4 wire.

The positions of the head-group Ru atom in the Λ and Δ C_4-wire complexes differ by ~3 Å. This difference ultimately stems from the enantiomeric arrangements of the bpy ligands and their interactions with protein surface residues, which cause the phen ligand in the Λ– and Δ–Ru(phen)$(bpy)_2$ head groups to have different preferred positions at the entrance to the active-site channel (Figure 3). Since the linker is a side chain of the phen ligand, the position of the phen affects the positions of the atoms in the linker. Further, the changes in the position of the head group and linker are accommodated by movements of the side chains of channel residues such as Glu102, Phe105 and Leu358. At the tail end of the wire, the differences between the Λ– and Δ–C_4-wire complexes disappear, and the interactions of the DMA tail group with the TPQ cofactor and other residues in the active-site cavity are closely similar (Supplementary Table S1). The DMA tail group is anchored primarily through hydrophobic interactions with the active-site cavity (Figure 4). The contacts between the DMA methyl groups and the O5 (TPQ) atom are 3.1–3.7 Å, and the angle between the DMA and TPQ aromatic ring planes is consistently ~70°. Similar contacts between the DMA tail group and the TPQ quinone ring occur in all the complexes of AGAO with a racemic C_5-C_{11} wire.

Inhibitor binding as a trigger for active-site conformational changes

All the AGAO-wire complexes reported here have their TPQ in an ‘off-Cu’ conformation. The occurrence of the TPQ cofactor in a single conformation is in contrast with the disorder that characterizes the TPQ cofactor in native AGAO.[6] The off-Cu conformation has previously been observed in AGAO derivatives where the TPQ is linked covalently to an inhibitor as the result of a chemical reaction. Indeed, the TPQ must be off-Cu for the formation of a covalent link to a ligand, be it an inhibitor or a substrate during the catalytic cycle. The AGAO-wire complexes are the first CuAO complexes in which the interaction between the TPQ cofactor and an inhibitor is non-covalent. We conclude that the insertion of a foreign molecule – the wire – that fits into the active site is all that is required to trigger the change of the TPQ to its off-Cu conformation.

A second protein residue that has different conformations in the absence or presence of a ligand in the active-site channel is Tyr296, the so-called ‘gate’. When the structure of AGAO is determined in the absence of a substrate or inhibitor, the Tyr296 gate is consistently ‘closed’. When a substrate or inhibitor is present, the closed conformation is sterically forbidden, and the gate is consistently ‘open’. Again, the open conformation of Tyr296 is essential to permit the entry of a ligand into the active site, and may well be triggered by that ligand.

Since the TPQ cofactor and Tyr296 gate can each exist in two alternative conformations, there are four possible combinations. One combination is sterically forbidden, and only two of the other three have been observed in crystal structures:

Gate	TPQ	Occurrence
Open	Off-Cu	AGAO derivatives with a ligand at active site
Closed	Off-Cu	Forbidden by steric overlap
Open	On-Cu	Permitted, but not observed
Closed	On-Cu	Native AGAO (TPQ may be disordered)

When a ligand enters the active-site channel and triggers the change to an ‘open gate, off-Cu TPQ’ conformation, the expulsion of bound water molecules from the channel results in an entropic contribution to the driving force. Additionally there is an enthalpic contribution from the new wire-protein contacts. The off-Cu conformation of the TPQ is further stabilized by a new hydrogen bond from the TPQ to a conserved Tyr residue, (TPQ)O4···O$^{\eta}$ (Tyr284). Similar hydrogen bonds occur in two earlier AGAO-inhibitor derivatives.[22] (We calculate close contacts of 2.4Å from PDB entries 1sii and 1sih). The corresponding hydrogen bond in *E. coli* amine oxidase, (TPQ)O4···O$^{\eta}$ (Tyr369), has been identified by Mure *et al*. as “controlling the position and orientation of TPQ in the catalytic cycle, including optimal orientation for reactivity with substrates”.[23]

Systematic trends in the linker and head-group regions

In the Λ- and Δ-C_4-wire complexes, the electron density representing the hydrocarbon linker segment of the wire is significant and continuous. In the complexes with racemic ligands, the corresponding electron density is weak or absent. As the length of the linker increases, the amplitude of the anomalous scattering difference assigned to the Ru atom decreases (Table 2).

These trends can be explained as follows. First, the racemic wire complexes have at least two components with slightly different structures, so that the electron density is weakened by disorder. Accordingly, in comparison with the Λ- and Δ- C_4 wires, the electron density of the racemic C_5-C_{11} wires is observably weaker. Second, the longer the linker segment of the wire, the less the Ru head group is restrained; and the weaker the restraints on the Ru head group, the greater is the disorder in the linker segment. While the distance from the enzyme active site to the Ru head group increases with the length of the linker segment (the C_7 wire being slightly out of order), the interactions between the head group and residues on the protein surface vary from wire to wire. Each Ru head group finds its own preferred position(s). Third, the C_4-wire complexes have a structural advantage, since the Ru head group is approximately level with the boundary of the AGAO molecule. Regardless of whether it is Λ or Δ, the head group fits into the end of the active-site channel, rather like a cork might fit into a bottle. The head group makes tight contacts with several of the nearest-neighbor protein residues. In the longer wires, such favorable complementarity is missing.

[DMA-C_n-Ru(phen)bpy$_2$] wires as specific amine oxidase inhibitors

In earlier work, we showed that wires of the type [DMA-C_n-Ru(phen)bpy$_2$] are powerful inhibitors of AGAO.[2] The kinetics measurements in ‘Results’ now provide evidence that the inhibition of AGAO by the [DMA-C_4-Ru(phen)bpy$_2$] wire is competitive. The most straightforward explanation of such inhibition is that the binding of the wire prevents access by substrate amines to the active site, consistent with the structural findings. However, some aspects of the inhibition deserve further comment.

Since AGAO discriminates structurally between the enantiomers of the C_4 wire, it is surprising that the Λ and Δ enantiomers and the racemic form of the C_4 wire have approximately the same effectiveness as inhibitors of amine oxidation. In other words, the effectiveness of the wire as an inhibitor is independent of the chirality of the Ru(phen)bpy$_2$] head group, implying that the chiral Ru head group does not control what happens in the rest of the wire molecule. To understand the function of the wire we have to concentrate on the linker and the DMA tail group, and on their relationships to residues lining the active-site channel and pocket of the enzyme. The alkane linker segment of the wire responds to the steric restrictions within the active-site channel, while the contacts between the DMA tail group and residues in the active-site pocket are identical or closely similar in all the complexes of AGAO and a [DMA-C_n-Ru(phen)bpy$_2$] wire. When AGAO is complexed with the enantiopure Λ- and Δ-C_4 wires, the potential interactions between the protein and the linker or the DMA tail group are predominantly hydrophobic (Figure 4).

The situation is complicated by the fact that the related enzyme ECAO discriminates between the Λ and Δ enantiomers of the C_4 wire more effectively than AGAO, but that the inhibition is only ~10% as effective. The racemic C_4 wire inhibits another related enzyme, BPAO, even less effectively, and two other related enzymes, PSAO and PPLO, are not inhibited at all. In the absence of relevant crystal structures, we speculate that all these observations may be explained by considering the active-site channel of each enzyme. The reduced effectiveness of the Λ and Δ C_4 wires as inhibitors of ECAO, and the enhanced ability of ECAO to discriminate between the wire enantiomers, may both be symptoms of a sterically more restrictive active-site channel. The active-site channel in PSAO may be sterically so restrictive that the wire is not bound; and conversely, the wide-open active-site channel in PPLO[16,24] may simply fail to provide sufficient specific interactions with the wire to cause effective binding and inhibition. The active-site channel in BPAO is also considered to be wide, but is omitted from this discussion since some relevant residues are disordered in the molecular model.[25]

Further comments on the importance of the wire head group

Finally, the present work shows that head-group electrostatic charge does not play a major role in wire binding. A search of the structures of all the racemic wire complexes shows that the protein side chains closest to the Ru atom are consistently Glu102 (at 5–10 Å), Glu106 (at 7–11 Å), and Arg336 (at 8–11 Å). In the structures of the Λ- and Δ-C_4-wire complexes, the [Ru(phen)(bpy)$_2$]$^{2+}$ head group is packed against the protein. The occupancy of the Ru head group is higher when the nearest neighbors are Glu102 and Arg336 (total charge 0) than when they are Glu102 and Glu106 (total charge −2), suggesting that side-chain electrostatic charges make relatively unimportant contributions to the head-group/protein interactions. Consistent with these observations, the C_4 wire with a Co^{III} head group is slightly *less* effective as an inhibitor of AGAO than the same wire with a Ru^{II} head group, despite the increased positive charge. From a design standpoint, it is likely that the effectiveness of a metal in a wire inhibitor depends less on the oxidation state of the metal than on the size, shape and inertness of the resulting head group, as well as the contribution that the head group makes to the solubility of the wire.

Conclusions

Molecular wires of the form [DMA-C_n-Ru(phen)(bpy)$_2$]$^{2+}$ are powerful competitive inhibitors of AGAO. A wire with n = 4 is particularly effective: when its DMA tail group occupies the active-site pocket, its Ru head group neatly plugs the entrance to the active-site channel. The enzyme discriminates structurally between the Λ- and Δ-enantiomers of the wire: In the crystal structures of the Λ- and Δ-C_4 wire complexes with AGAO, the chiral Ru head group occupies different positions with respect to the protein surface, and there are small differences between

the conformations of the alkane linker segment. These properties of the C_4-wire complexes help to rationalize our observations on the complexes of AGAO with longer wires, and on the complexes of the C_4 wire with several other copper amine oxidases.

In summary, we report that inhibition by a 'wire-type' compound can be remarkably selective, and that the selectivity is created by multiple interactions between the inhibitor and the enzyme. There are strong indications that the critical interactions are located within the active-site cavity and the active-site channel. Thus, the composition and dimensions of the tail group and linker of the wire have to complement the dimensions, shape and surface properties of the cavity and channel of the protein. These are useful clues for the design of inhibitors with therapeutic applications. In the long term, many such applications depend on the ability to inhibit an enzyme in a pathogen, without inhibiting analogous enzymes in the host. Since access to the active site of many enzymes is provided by a sterically restrictive channel, a strategy that exploits the structural properties of such channels in the design of specific inhibitors may be widely applicable.

Supplementary Material

Refer to Web version on PubMed Central for supplementary material.

Acknowledgments

We thank Nick Halpern-Manners and Alexander Dunn for assistance in the early stages of this work. The work was supported by the National Institutes of Health (DK19038 to H.B.G, GM27659 to D.M.D.) and the Australian Research Council (DP0208320 to J.M.G. and H.C.F.).

References

1. Hess CR, Juda GA, Dooley DM, Amii RN, Hill MG, Winkler JR, Gray HB. J. Amer. Chem. Soc 2003;125:7156–7157. [PubMed: 12797771]
2. Contakes SM, Juda GA, Langley DB, Halpern-Manners N, Duff AP, Dunn AR, Gray HB, Dooley DM, Guss JM, Freeman HC. Proc. Nat. Acad. Sci. USA 2005;102:13451–13456. [PubMed: 16157884]
3. Hua X, von Zelewski A. Inorg. Chem 1995;34:5791–5797.
4. Juda GA, Bollinger JA, Dooley DM. Protein Expression Purif 2001;22:455–461.
5. Otwinowski, Z.; Minor, W. Methods in Enzymology. Carter, CW.; Sweet, RM., editors. Vol. 276. New Yrok: Academic Press; 1997. p. 307-326.Macromolecular Crystallography, Part A
6. Langley DB, Duff AP, Freeman HC, Guss JM. Acta Crystallogr 2006;F62:1052–1057.
7. Winn MD, Isupov MN, Murshudov GN. Acta Crystallogr 2001;D57:760–763.
8. Van Aalten DMF, Bywater R, Findlay JBC, Hendlich M, Hooft RWW, Vriend G. J. Comp. Aid. Mol. Des 1996;10:255–262.
9. Murshudov GN, Vagin AA, Dodson EJ. Acta Crystallogr 1997;D53:240–255.
10. Laskowski RA, MacArthur MW, Moss DS, Thornton JM. J. Appl. Crystallogr 1993;26:283–291.
11. Davis IW, Murray LW, Richardson JS, Richardson DC. Nucleic Acids Res 2004;32:W615–W619. [PubMed: 15215462]
12. DeLano, WL. The PyMOL Molecular Graphics System. San Carlos, CA, USA: DeLano Scientific LLC; 2002.
13. Matsuzaki R, Fukui T, Sato H, Ozaki Y, Tanizawa K. FEBS Lett 1994;351:360–364. [PubMed: 8082796]
14. Saysell CG, Murray JM, Wilmot CM, Brown DE, Dooley DM, Phillips SEV, McPherson JM, Knowles PF. J. Mol. Catalysis B: Enz 2000;8:17–25.
15. McGuirl MA, McCahon CD, McKeown KA, Dooley DM. Plant Physiol 1994;106:1205–1211. [PubMed: 7824646]
16. Duff AP, Cohen AE, Ellis PJ, Kuchar JA, Langley DB, Shepard EM, Dooley DM, Freeman HC, Guss JM. Biochemistry 2003;42:15148–15157. [PubMed: 14690425]

17. Suzuki S, Sakurai T, Nakahara A, Manabe T, Okuyama T. Biochemistry 1983;22:1630–1635. [PubMed: 6303389]

18. Neumann R, Hevey R, Abeles RH. J. Biol. Chem 1975;250:6362–6367. [PubMed: 1171863]

19. Tabor CW, Tabor H, Rosenthal SM. J. Biol. Chem 1954;208:645–661. [PubMed: 13174575]

20. Lee Y, Shepard E, Smith J, Dooley DM, Sayre LM. Biochemistry 2001;40:822–829. [PubMed: 11170400]

21. Segel. Enzyme kinetics: Behavior and analysis of rapid-equilibrium and steady-state enzyme systems. New York: John Wiley and Sons; 1975.

22. O'Connell KM, Langley DB, Shepard EM, Duff AP, Jeon H-B, Sun G, Freeman HC, Guss JM, Sayre LM, Dooley DM. Biochemistry 2004;43:10965–10973. [PubMed: 15323556]

23. Mure M, Kurtis CRP, Brown DE, Rogers MS, Tambyrajah WS, Saysell C, Wilmot CM, Phillips SEV, Knowles PF, Dooley DM, McPherson JM. Biochemistry 2005;44:1583–1594. [PubMed: 15683242]

24. Duff AP, Cohen AE, Ellis PJ, Hilmer K, Langley DB, Dooley DM, Freeman HC, Guss JM. Acta Crystallogr 2006;D62:1073–1084.

25. Lunelli M, Di Paolo ML, Biadene M, Calderone V, Battistuta R, Scarpa M, Rigo A, Zanotti G. J. Mol. Biol 2005;346:991–1004. [PubMed: 15701511]

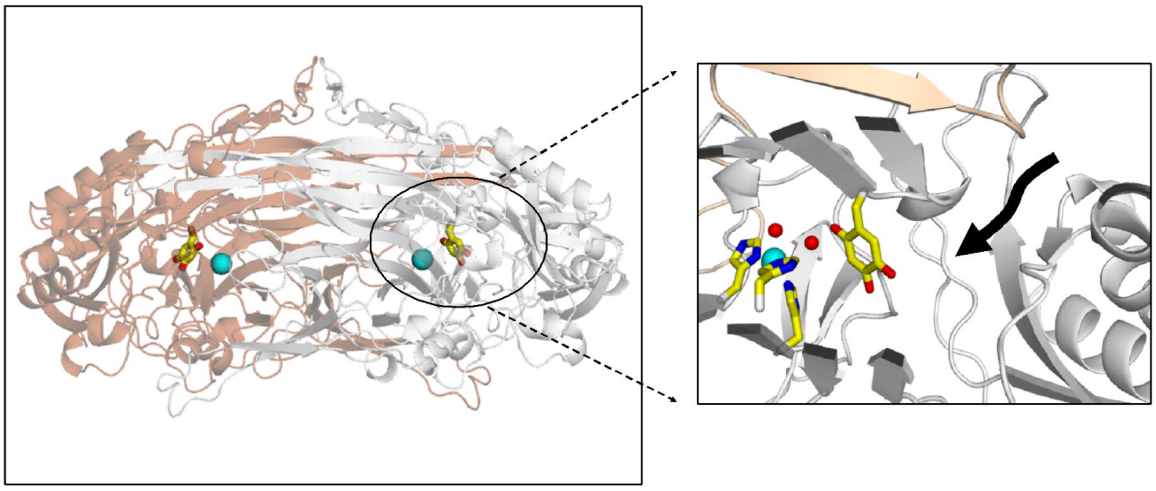

Figure 1.
(*Left*): Ribbon diagram of an *Arthrobacter globiformis* amine oxidase (AGAO) molecule. The colors distinguish the two protomers of the homodimer. The Cu atoms are shown as blue spheres.
(*Right*): The active site, showing the TPQ side chain in the 'off-Cu' conformation. The red spheres are H_2O molecules coordinated to the Cu atom. The black arrow indicates the direction of the channel along which substrates pass from the molecular surface to the active site.

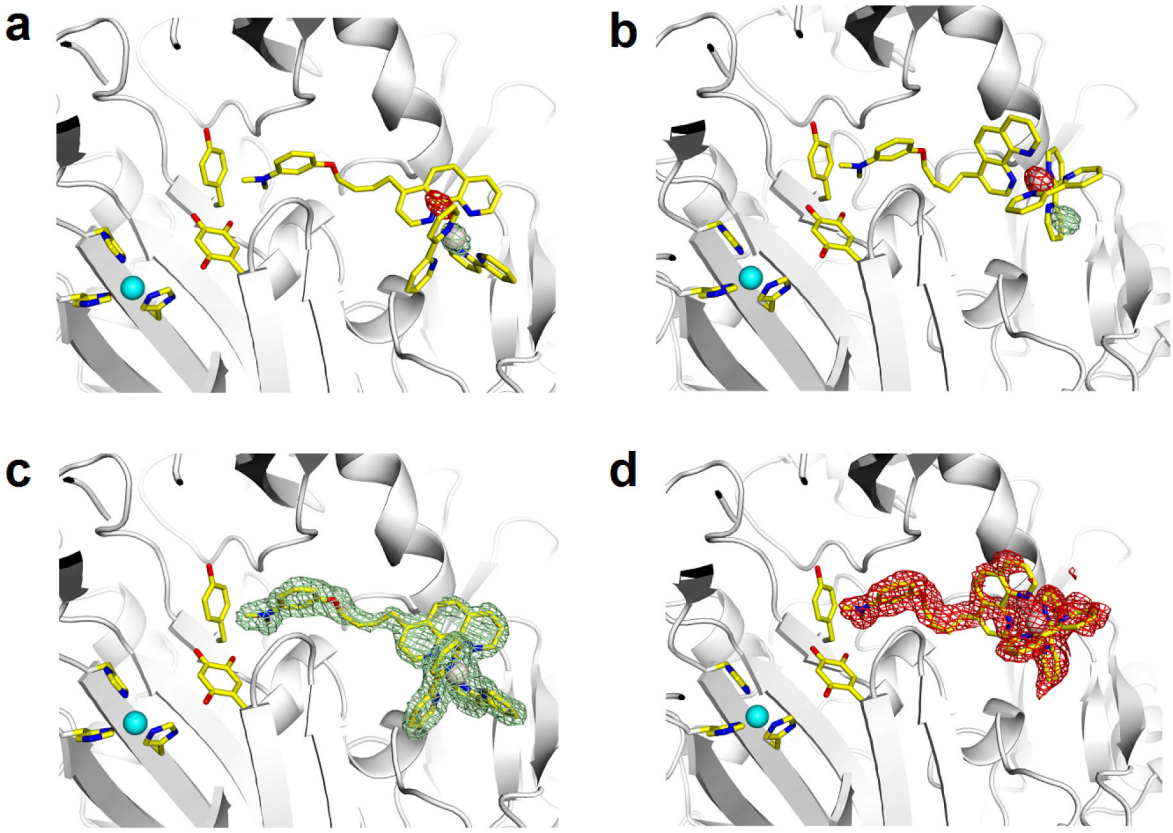

Figure 2. Models and electron density of the Λ- and Δ-[(DMA-C_4-Ru(II)(phen)bpy)2] wires in the active-site channel of AGAO

Each diagram includes the active-site Cu atom with its three His ligands, the TPQ cofactor, and the Tyr296 'gate' residue. *(a)* and *(b)*: Models of the Λ- and Δ-C_4-wires, as seen in the structures of the enantiopure complexes. The red and pale-green 'mesh' contours show the two anomalous scattering difference peaks from the structure analysis of the racemic C_4-wire complex. *(c)* and *(d)*: Electron-density ($2F_{obs} - F_{calc}$) contours for the Λ- and Δ-C_4-wires in the enantiopure complexes. The pink and blue spheres represent the Ru and Cu atoms, respectively.

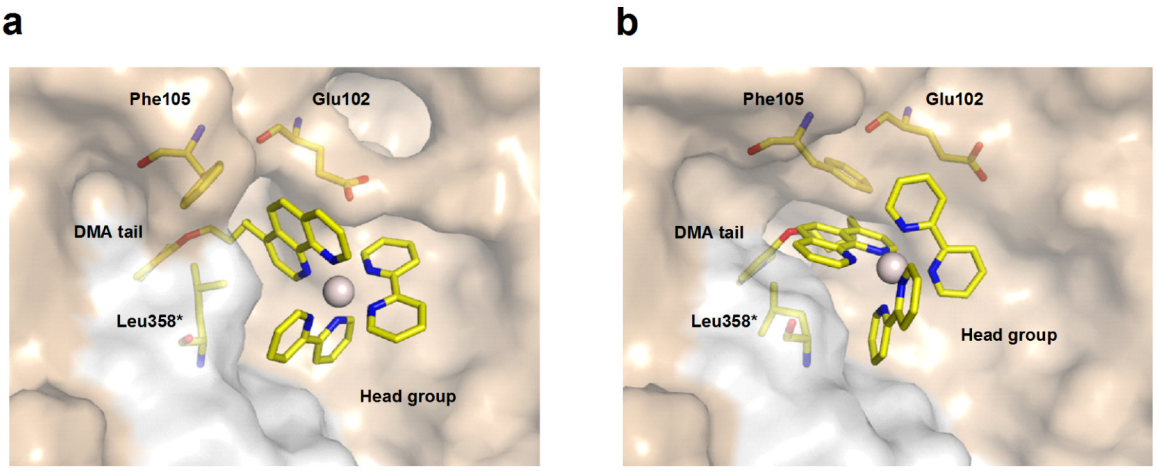

Figure 3. The Ru(II) head groups of the enantiomeric C_4-wires at the entrance to the AGAO active-site channel

(a) Head group of the Λ-C_4-wire. *(b)* Head group of the Δ-C_4-wire. The side chains of Glu102, Phe105 and Leu358* adopt different conformations in response to the binding of the enantiomeric wires. The asterisk on L358* reminds us that this channel residue belongs to the second subunit of the dimer. The surface of the active-site channel is drawn in two colors to indicate that both protomers of the homodimeric AGAO molecule contribute to the channel.

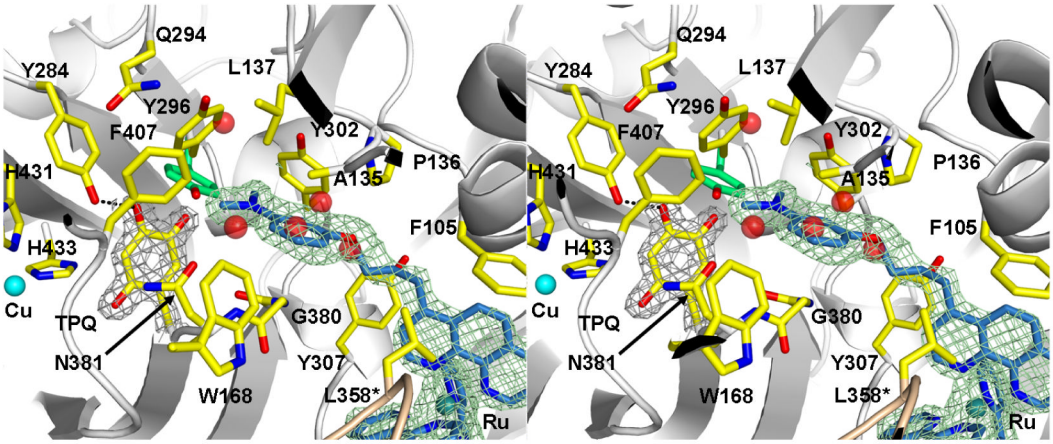

Figure 4. The tail group of the Λ-C_4 wire in the active-site pocket of AGAO

The tail of the Λ-C_4 wire (blue) is shown inside the green 'mesh' contours ($2F_{obs}$-F_{calc} difference density at 1.0σ), and the TPQ is shown inside the grey 'mesh' contours ($2F_{obs}$-F_{calc} difference density at 2.0σ). The active-site 'gate' tyrosine (Y296) is drawn in two conformations – open (yellow, present work) and closed (green, PDB entry 1w6g). The AGAO residues that make Van der Waals contact with the linker or tail group of a wire are: Phe105, Ala135, Pro136, Leu137, Trp168, Tyr296 (the 'gate'), Tyr302, Tyr307, Leu358*, Gly380 and TPQ382. The channel residue L358* belongs to the second subunit of the dimer. An important hydrogen bond between TPQ and Tyr284 is shown as a dotted line. Water molecules displaced from the channel by the wire are shown as red spheres.

The $–N(CH_3)_2$ group of the DMA (blue) is in contact with the TPQ quinone ring, which is in the off-Cu conformation. The 'gate' residue, Y296, is restricted to its open conformation by the presence of the wire. In the absence of a substrate or other ligand, the gate would typically be in the closed conformation (green).

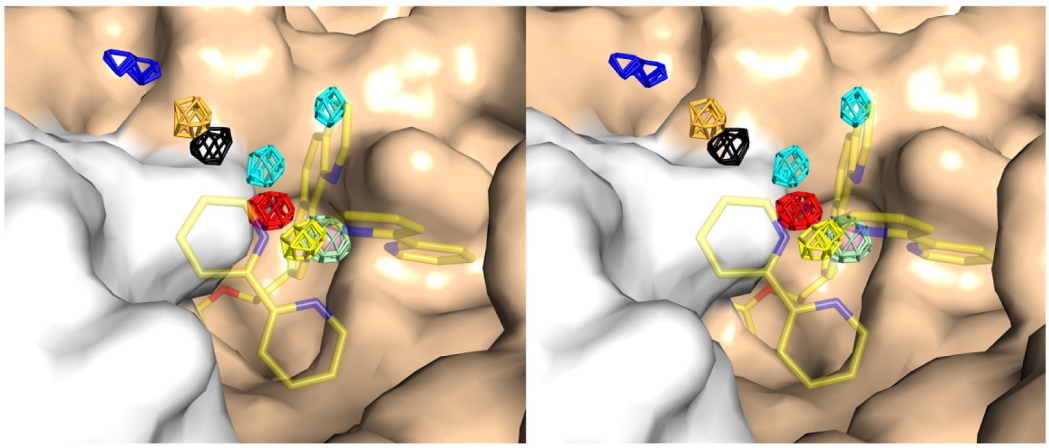

Figure 5. Stereo view of the major Ru sites in relation to the surface of the protein molecule

The colored contours indicate the major anomalous scattering difference peak(s) from each structure analysis. *Pale green*: Λ-C_4-wire. *Red*: Δ-C_4-wire. *Cyan*: Racemic C_5-wire. *Black*: Racemic C_6-wire. *Yellow*: Racemic C_7-wire. *Orange*: Racemic C_9-wire. *Blue*: Racemic C_{11}-wire. The Λ-C_4-wire can be seen in the active-site channel below the magenta Ru peak. Minor peaks are omitted.

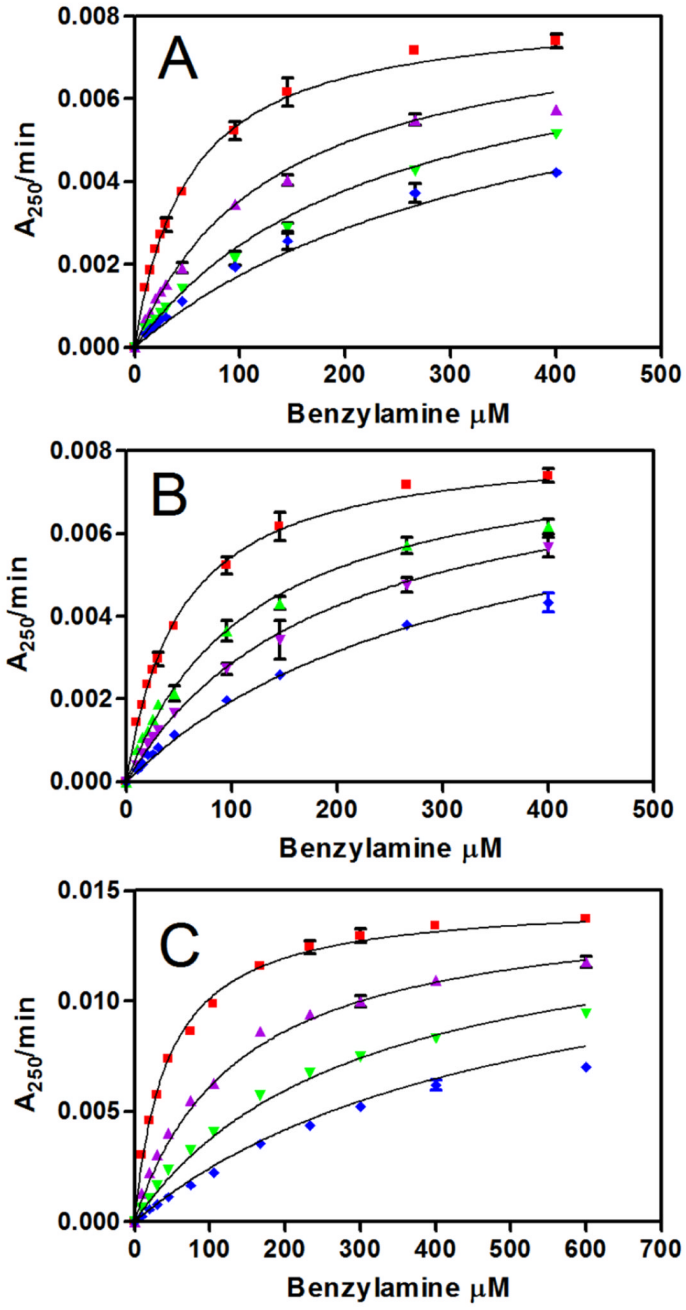

Figure 6. Inhibition of AGAO by racemic, Λ- and Δ-compounds

The curves are global fits for a competitive model. Concentrations of inhibitor: (A) Racemic - control, 42 nM, 95 nM, 168 nM. (B) Λ-control, 42 nM, 84 nM, 168 nM. (C) Δ-control, 77 nM, 202 nM, 374 nM. Error bars represent the standard deviation of the rate at the given benzylamine concentration.

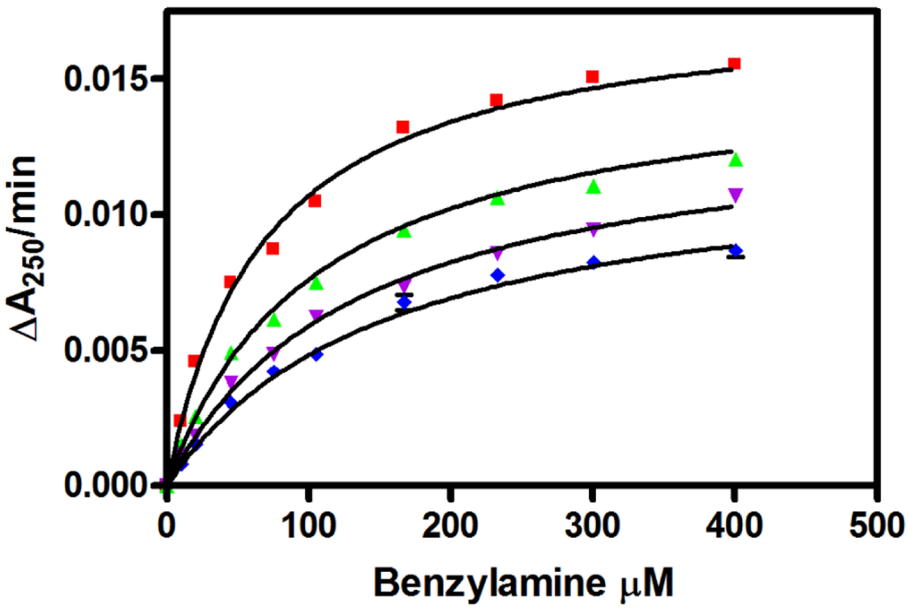

Figure 7. Inhibition of AGAO by a racemic Co^{III} C_4 wire

The curves are global fits for a mixed-type inhibition model with K_i = 120 ± 4.3 10^{-9} M (R^2 = 0.996). Error bars represent the standard deviation of the rate at the given benzylamine concentration.

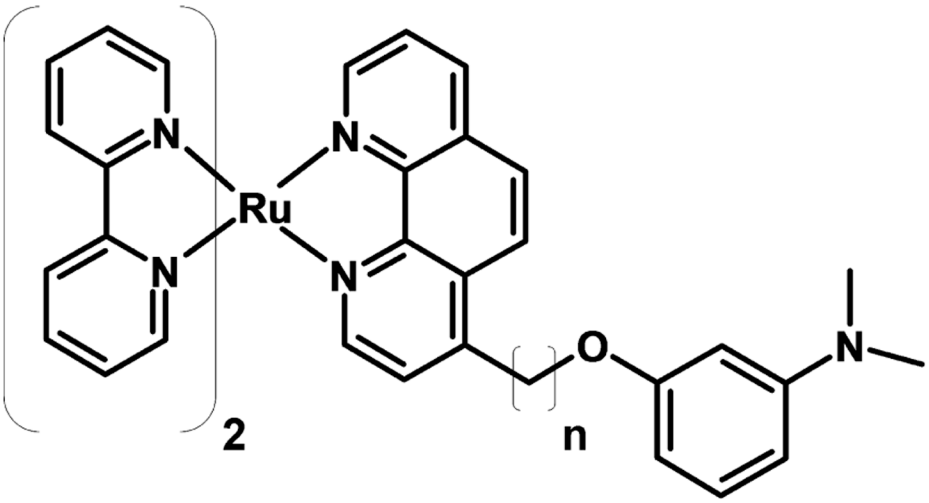

Scheme.
Formula of DMA–$(CH_2)_n$–$[Ru(phen)(bpy)_2]^2$ wire.

Table 1

Crystallographic and refinement data. The length of each wire is indicated by 'C_n', where n is the length of the –$(CH_2)_n$– linker in DMA–$(CH_2)_n$–$[Ru(phen)(bpy)_2]^{2+}$. The chirality of the head group is shown in parentheses. Numbers in parentheses refer to the tenth (outer) shell of the diffraction data.

Wire	**C_4 (Λ)**	**C_4 (Δ)**	**C_4 (racemic)**	**C_5 (racemic)**	**C_6 (racemic)**	**C_7 (racemic)**	**C_9 (racemic)**	**C_{11} (racemic)**
Space group	*I*2	*I*2	*C*2	*C*2	*C*2	*C*2	*C*2	*C*2
Molecules/ asymmetric unit	2	2	1	1	1	1	1	1
a, *b*, *c* (Å)	192, 63, 158	192, 63, 158	158, 63, 92	158, 63, 92	158, 63, 92	158, 63, 92	158, 63, 92	158, 63, 92
β (°)	117.5	117.5	112.1	112.2	112.2	112.1	112.2	112.2
Resolution (Å)	1.60	1.55	1.73	1.80	1.80	1.74	1.80	1.67
I/sig(I)	9.5 (3.2)	10.5 (1.6)	22.5 (5.8)	24.4 (4.3)	24.6 (3.4)	22.8 (4.2)	20.4 (3.9)	23.9 (5.1)
R_{merge}	0.04 (0.28)	0.04 (0.41)	0.04 (0.11)	0.03 (0.15)	0.04 (0.19)	0.04 (0.23)	0.04 (0.23)	0.03 (0.16)
Multiplicity	5 (3.8)	5.3 (4.2)	3.9 (2.7)	4.2 (2.6)	6.4 (2.9)	4 (3.6)	3.9 (3.5)	3.6 (3.2)
No. of unique reflections	196,351	214,120	77,947	72,905	70,735	76,355	68,517	89,939
Completeness	0.939	0.926	0.945	0.989	0.958	0.929	0.925	0.973
Wilson *B* ($Å^2$)	21	23	20	22	27	22	25	20
Mean *B* ($Å^2$)	21.4	27.6	15.6	22.0	29.1	22.9	29.7	22.7
No. of non-H atoms	10,561	10,741	5,553	5,489	5,374	5,387	5,309	5,442
Rms Δ bonds (Å)	0.011	0.011	0.011	0.01	0.012	0.01	0.01	0.009
Rms Δ angles (°)	1.46	1.45	1.53	1.51	1.49	1.47	1.46	1.39
Rms Δ peptide planarity (°)	6.52	6.30	6.19	6.26	6.42	6.29	6.29	6.16
R	0.194	0.203	0.154	0.145	0.156	0.161	0.167	0.160
R_{free}	0.213	0.224	0.171	0.165	0.178	0.176	0.186	0.179
ESU (Å)	0.084	0.082	0.087	0.087	0.095	0.091	0.110	0.077
PDB Reference	2cfd	2cfg	2bt3	2cfk	2cfl	2cfw	2cg0	2cg1

Table 2

Anomalous scattering difference peaks for Ru atoms, scaled with respect to the corresponding peak for S(Met441).[1]

Wire →	C_4 (Λ) A chain	C_4 (Λ) B chain	C_4 (Δ) A chain	C_4 (Δ) B chain	C_4 (racemic)	C_5 (racemic)	C_6 (racemic)	C_7 (racemic)	C_9 (racemic)	C_{11} (racemic)
Amplitude of S (Met441) peak[2]	10.6	14.7	8.3	10.4	14.3	12.4	10.7	12.2	12.3	16.4
Amplitude of S (Met280) peaks[3]	5.2, 3.6	6.2, 5.5	6.3, 5.3	7.1, 4.3	7.0, 4.9	6.6, 4.4	5.5, 4.1	6.5, 4.6	4.4, 4.3	7.9, 7.5
Amplitude of Major Ru peak	29.0	33.9	13.6	17.8	14.6	9.7	7.4	8.4	6.5	4.5
Amplitude of Minor Ru peaks	-	3.2	5.6	6.0, 5.1[4]	7.6	8.5	3.9	5.2, 3.7	4.9	-
Scaled Major Ru peak[5]	2.7	2.3	1.6	1.7	1.0	0.8	0.7	0.7	0.5	0.3
Scaled Minor Ru peaks[5]	-	0.2	0.7	0.6, 0.5	0.5	0.7	0.4	0.4, 0.3	0.4	-
Scaled S (Met280) peaks,[35]	0.5, 0.3	0.4, 0.4	0.8, 0.6	0.7, 0.4	0.5, 0.3	0.5, 0.4	0.5, 0.4	0.5, 0.4	0.4, 0.3	0.5, 0.5
Refined occupancy of Ru site[6]	0.7	0.7	0.5	0.5	0.3	0.2	0.2	0.5	0.5	0.2

[1] A typical anomalous scattering difference map had peaks at the positions of the Cu atom, the sulfur atoms of residues Met441 and Met280, and the Ru atom.

[2] The peak representing S(Met441) was used as a standard, since the side chain of this residue was well ordered in all known AGAO structures (including the present ones).

[3] The S(Met280) atom was observed as two weak peaks consistent with the presence of two side-chain conformers. The amplitude of the weaker peak provided a conservative indicator of the noise level of the map.

[4] The presence of a second minor peak in one subunit is unexplained.

[5] The amplitudes of all peaks are expressed as a multiple of the amplitude of the S(Met441) peak.

[6] The occupancies of the Ru site were refined as described in ‘Materials and methods’. Theoccupancies of the DMA tail group were constrained as 1.0.

Table 3

Distances between the TPQ cofactor of the enzyme and the Ru head group of the wire

Wire type	**Λ**	**Δ**			**Racemic**		
Linker length, *n*	4	4	5	6	7	9	11
d[O5(TPQ)–Ru], Å	15.6	14.5	17.0*	18.0	16.6	19.3	22.1

* Average of distances to two approximately equal Ru peaks (see Table 2)

Table 4

K_i values for the inhibition of benzylamine oxidation.

CuAO	C_4 Wire	K_i	Type of Inhibition
AGAO	racemic	27 ± 1 nM	Competitive
AGAO	Λ	32 ± 1 nM	Competitive
AGAO	Δ	36 ± 2 nM	Competitive
AGAO	Co^{III}	120 ± 4 nM	Mixed
ECAO	Λ	0.27 ± 0.02 μM	Competitive
ECAO	Δ	1.10 ± 0.08 μM	Competitive
BPAO	racemic	44 ± 4 μM	Non-competitive
PPLO	racemic	-	No inhibition
PSAO	racemic	-	No inhibition